Hindawi Publishing Corporation
International Journal of Photoenergy
Volume 2014, Article ID 406495, 10 pages
http://dx.doi.org/10.1155/2014/406495

Research Article

Growth and Properties of ZnO:Al on Textured Glass for Thin Film Solar Cells

Marta Lluscà,[1] Aldrin Antony,[1,2] and Joan Bertomeu[1]

[1] *Department of Applied Physics and Optics, Universitat de Barcelona, 08028 Barcelona, Spain*
[2] *Department of Energy Science and Engineering, Indian Institute of Technology Bombay, Mumbai 400076, India*

Correspondence should be addressed to Marta Lluscà; marta.llusca@ub.edu

Received 18 June 2014; Revised 31 July 2014; Accepted 31 July 2014; Published 28 August 2014

Academic Editor: Raghu N. Bhattacharya

Aluminium induced texturing (AIT) method has been used to texture glass substrates in order to enhance the photon absorption in thin film solar cells. The resultant glass roughness has been analyzed by varying the AIT process parameters and it has been found that the deposition method of Al is a decisive factor in tuning the texture. Two types of textures, a soft (texture E) and a rough texture (texture S), were achieved from the thermally evaporated and sputtered Al layers through AIT process. Aluminium-doped zinc oxide (AZO) layers of different thickness were deposited over both textures and over smooth glass. Haze values above 30% were obtained for texture S + AZO and above 10% for texture E + AZO. The resultant morphologies were free from sharp edges or deep valleys and the transparency and the resistivity values were also good enough to be used as front contact for thin film solar cells. In order to demonstrate the light absorption enhancement in a solar cell device, 200 nm of a-Si:H followed by 300 nm of Ag were grown over the textured and smooth substrates with AZO, and an optical absorption enhancement of 35% for texture E and 53% for texture S was obtained in comparison to the smooth substrate.

1. Introduction

Use of textured and conducting front contacts in thin film silicon solar cells enhance photon absorption in active layers. Thanks to index grading which decreases the reflection losses and light trapping mechanism by the scattering at the textured front surface, the net result is an increased optical path for the incident light [1]. Texturing of glass substrate is an interesting alternative to enhance light trapping instead of using conventional naturally textured transparent conducting oxides such as ZnO:B grown by LPCVD [2], SnO_2:F grown by APCVD [3], or through HCl etching of sputtered ZnO:Al (AZO) [4]. In this work, the texturing of the glass substrate by aluminium induced texturing (AIT) as an alternative to improve optical behaviour of thin film solar cells is studied as well as the growth of sputtered AZO over these textured glass surfaces.

AIT is a method to texture glass surface, which is based on a thermally activated chemical reaction between the glass and a thin Al layer deposited either by sputtering or evaporation method [5]. The high temperature during the thermal annealing of the Al coated glass favours a spatially non-uniform redox reaction according to the following equation:

$$4Al + 3SiO_2 \longrightarrow 2Al_2O_3 + 3Si \quad (1)$$

Followed by this thermal annealing, the reaction products (Al_2O_3 and Si) are removed by a wet chemical etching and the result is a rough and uniform texture over the glass surface.

It has been demonstrated that the final roughness can be controlled by varying the process parameters such as the etching solution [5, 6], the etching time [7], initial Al thickness [8], and annealing conditions [7]. The AIT method can create a suitable substrate texture for polysilicon solar cells [5, 6, 8, 9] as well as for amorphous and microcrystalline thin film silicon solar cells [7].

In this work different types of textures have been achieved by varying the AIT process parameters such as Al thickness, annealing time, and etching temperature, but a special attention has been given to the Al deposition method that

resulted in very different textures if the Al was deposited by sputtering (texture S) or thermal evaporation (texture E). Moreover, different thicknesses of DC sputtered AZO have been deposited onto these textures. The surface morphology, structure, and optical and electrical properties of the resulting samples have been analysed in detail. It has been observed that a double texture based on a U-shape morphology is obtained for AZO deposited over texture E, presenting ~14% of haze at 600 nm with a sheet resistance of 7 Ω/□ (AZO thickness = 1000 nm); on the other hand for AZO deposited over texture S, the resultant morphology yielded a cauliflower surface texture with high haze values ~30% at 600 nm.

2. Experimental

Borofloat glass substrates of 2 mm thick were cautiously cleaned in an ISO 7 (10000 type) clean room. The cleaning process of the substrate was found to be a very critical step in the resulting uniformity and texture of the glass surface. The glass substrates were initially cleaned with detergent solution (Decon 90) followed by the ultrasonic cleaning for 15 minutes each in deionised water, isopropanol, and again in deionised water and then dried in nitrogen. To remove the humidity at the surface, the cleaned glasses were kept in a hot air oven at 120°C for 30 minutes.

Al was deposited at room temperature onto these cleaned substrates by thermal evaporation. The thickness of the evaporated Al films varied between 30 nm and 250 nm. Also a magnetron sputtering system was employed for the deposition of the Al film in order to compare the effect of different deposition methods. Al films of 250 nm thickness were deposited using an RF power of 150 W at a working pressure of 0.13 Pa without any intentional heating of the substrate. The samples were then annealed in air atmosphere in a quartz tubular furnace at 600°C between 10 minutes to 1 hour, allowing a chemical reaction between the glass substrate and the Al layer.

Removal of the Al layer and the reaction products was realized by immersing in hot (185°C) concentrated (85%) orthophosphoric acid (H_3PO_4). The immersion time was varied from the minimum time needed for the complete removal of the resultant layer (as determined from visual inspection) to 60 additional minutes, and the solution temperature was also varied from 160 to 210°C.

AZO thin films were deposited via DC magnetron sputtering onto the textured glass substrates. The films were deposited at a working pressure of 0.4 Pa, using a DC power of 200 W and keeping the substrate at a temperature of 300°C. The target used was ZnO/Al_2O_3 (98/2 wt%) of 3 inch diameter and 99.99% purity. The base pressure in the chamber was always below 7×10^{-4} Pa. AZO films of three different thicknesses 500 nm (AZO1), 700 nm (AZO2), and 1000 nm (AZO3) were deposited by varying the deposition time onto textured and smooth glass substrates. Further, amorphous silicon (a-Si:H) layers (200 nm) were deposited by RF PECVD over smooth and textured samples with 1000 nm of AZO. In order to study the effect of the texture on optical absorption, Ag of 300 nm was deposited by thermal evaporation to form a nonfunctional device structure, textured glass/AZO/a-Si:H/Ag.

Morphological characterization of the samples was performed using atomic force microscopy (AFM) and high resolution scanning electron microscopy (HRSEM). The atomic force microscope images were taken using a Pacific Instruments system and the software for data analyses was XEI 1.7.3 of Psia Inc. from which the rms roughness (σ_{rms}) and the power spectral density (PSD) values were obtained. The σ_{rms} values were calculated from the AFM images of $15 \times 15\ \mu m^2$ area. The HRSEM was done using a Nova NanoSEM from FEI electron microscope.

The crystallinity of the AZO films was analysed using X-ray diffraction method (PANalytical X'Pert PRO MPD Alpha1 powder system, using Cu K_α radiation, $\lambda = 1.5406$ Å). The average crystallite size of the films ($\langle D \rangle$) was calculated from the integral breadth using the following Scherrer formula:

$$\langle D \rangle = \frac{\lambda}{\beta \cos \theta}, \tag{2}$$

where β is the integral breadth, λ is the X-ray wavelength, and θ is the Bragg's angle of diffraction corresponding to the diffraction peak.

The transmittance (T), diffused transmittance (T_d), and reflectance (R) were recorded by using a spectrophotometer (Perkin Elmer Lambda 950) with a 150 mm integrating sphere.

The haze ratio (H) was calculated from the quotient between T_d and T following (3):

$$H = \frac{T_d}{T}, \tag{3}$$

and the absorbance (A) was deduced by using the T and R spectra according to the following equation:

$$A(\lambda) = 1 - T(\lambda) - R(\lambda). \tag{4}$$

The sheet resistance was measured by using a four-point probe system (Jandel RM3). To assess the quality of the transparent and conducting films, the figure of merit values were calculated according Haacke [10], using the relation,

$$\Phi = \frac{T^{10}}{R_s}, \tag{5}$$

where T is the integrated optical transmission in the range 400–800 nm, and R_s is the electrical sheet resistance in Ω/□.

3. Results and Discussion

The results are divided into two sections, the first one presents a study on the influence of the AIT parameters on the resultant glass texture, and the second section presents the characterization of different thicknesses of AZO grown on the textured substrates. The optical and electrical properties are critically evaluated based on the requirement to be used in silicon thin films.

3.1. AIT Process Parameters. To study the effect of annealing time and Al thickness on the glass texturisation process, Al layers of different thickness were evaporated on glass substrates and were annealed varying in the time and temperature. Independent of the thickness or the evaporation conditions, the minimum temperature to allow the reaction process to occur was ~600°C. The reaction usually started from the edges of the samples and propagated to the centre till the whole surface changed its aspect and became dark. The time needed for the complete reaction depends on the Al layer thickness. Figure 1 presents the σ_{rms} values estimated from the AFM pictures in $15 \times 15\,\mu m^2$ areas depending on the annealing time and the initial Al thickness. The furnace temperature was kept at 600°C and the reaction products were etched with hot H_3PO_4 until they were completely removed. The first point on each sample represents the minimum annealing time required to produce the reaction.

As seen in Figure 1, once the reaction has occurred no difference in σ_{rms} roughness was observed by increasing the time of annealing. This behaviour was also observed for the haze values of the samples (not shown here). In addition, it has been seen that soft textures were formed ($\sigma_{rms} \sim 15$ nm) for thicknesses < 50 nm due to the limited Al used, whereas for thicknesses > 50 nm, higher textures ($\sigma_{rms} \sim 45$ nm) can be achieved.

The etching solution that has been used is hot concentrated (85%) H_3PO_4 between 160°C and 210°C. Since water evaporates from the solution at this temperature range, the solution gets more concentrated and the etching rate increases and becomes difficult to control [11]. The minimum temperature required to etch the reaction products was observed to be 185°C, and the etching time depended on the initial Al thickness; thus thicker layers required more time for etching. Furthermore, the etching process above 210°C leads to the reaction of the solution with the glass, forming silicon phosphate spots and reducing the texture [12]. Although HF based solutions have been usually used to etch the reaction products [5, 7, 8], in this work no other acids than just hot H_3PO_4 were employed. The deposition method and the deposition parameters are critical for the resultant roughness. In the case of sputtering, the energy at which the Al adatoms reach the glass substrate is higher than with evaporation, and hence the Al films are better adhered to the substrate and grow more compact and even might be diffusing into the substrate [13, 14]. Moreover, since it is an interface reaction, the cleanliness of the surface is also extremely important. To study the effect of the deposition method on the final roughness, two samples with the same Al thickness (~250 nm) were prepared, one through thermal evaporation (texture E) and the other one via RF magnetron sputtering (texture S) without any substrate heating. Figure 2 shows the HRSEM micrographs of the resultant glass surface after applying the AIT method using both techniques. As seen in Figure 2(a), texture E showed U-shaped crater texture with crater size varying between 500 nm to 1.5 μm with σ_{rms} = 56 nm. The highly rough texture evolved for sample S (σ_{rms} = 145 nm) is assigned to the efficiency of the sputtering process to yield stronger adhesion and compact films in comparison with evaporation [13, 14], and for these films during the thermal annealing step of the AIT, the Al atoms might have diffused deeper into the glass surface.

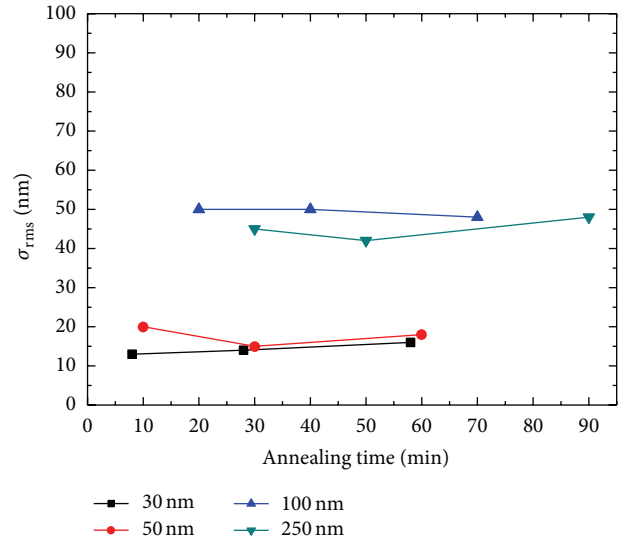

FIGURE 1: σ_{rms} values estimated from AFM over $15 \times 15\,\mu m^2$ images for different annealing time and Al thickness.

Figure 3 shows the haze values of Borofloat glass substrates with textures E and S. It is seen that the haze value reaches 35% for texture S and 15% for texture E at $\lambda = 600$ nm. Moreover, the integrated transmittance of these samples in the range 400–800 nm was above 91%.

3.2. Properties of AZO on Textured Glass Substrates. To study the influence of the glass texture on the growth of AZO, three different thicknesses of AZO (500 nm, 700 nm, and 1000 nm) were deposited via DC magnetron sputtering onto a smooth glass surface and on textures E and S. HRSEM and AFM have been used to evaluate the morphology, and XRD measurements were employed to characterize the structure. Optical and electrical properties have also been analysed.

The characteristic texture of the sputtered AZO depends on the deposition conditions [15] and thickness [16]. According to the Thornton model, at higher deposition pressures and lower temperatures, higher roughness and less compact layers are formed [15]. Since, in this work, it was prioritized to get better conductivity, transparency, and compactness than higher roughness values for TCO; sputtering conditions of high substrate temperature and low working pressure were used to yield films having soft textures of $\sigma_{rms} \sim 5$–9 nm on smooth substrates.

Figure 4 shows the HRSEM micrographs of texture E and its combination with 500 nm, 700 nm, and 1000 nm of AZO. It can be seen that the samples with AZO over texture E show a double texture based on U-shaped interconnected craters of about 1 μm in size with nanoscale etching pattern spread over the surface (Figures 4(b), 4(c), and 4(d)). The nanoscale pattern that is observed over the craters could be due to the presence of a minor roughness that might have formed during the AIT process (not appreciable in HRSEM micrograph of

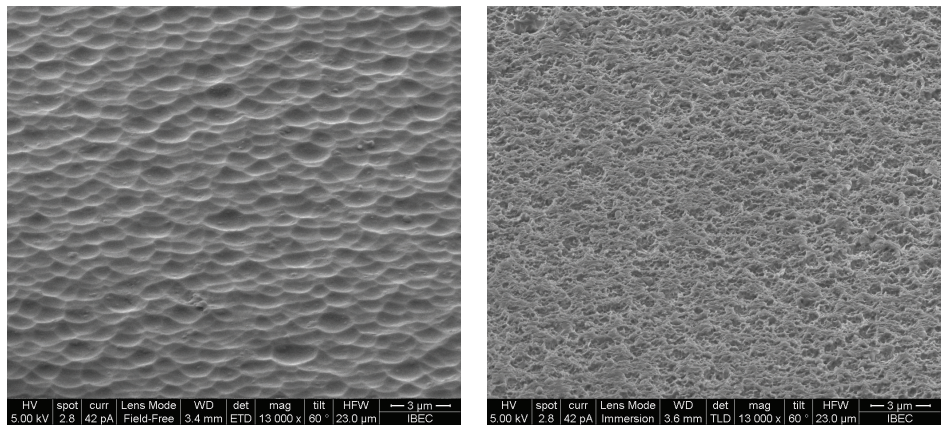

(a) (b)

Figure 2: HRSEM micrographs (tilted at 60°) of textured glass surfaces (a) texture E and (b) texture S.

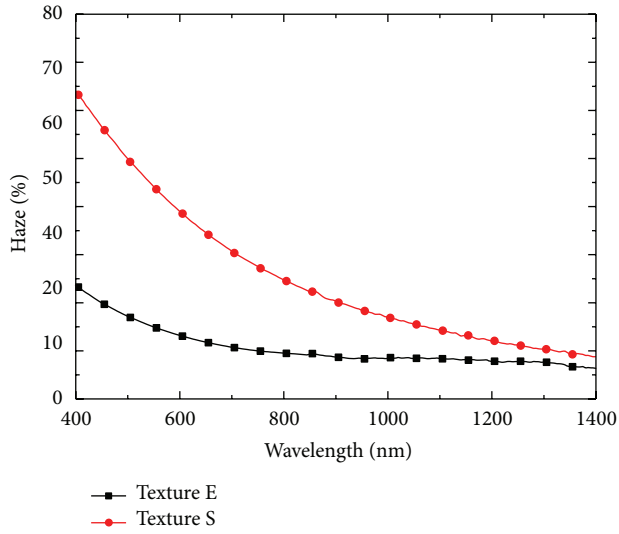

Figure 3: Haze of texture E and texture S.

texture E) and became pronounced with the growth of AZO deposition and/or due to the columnar growth over tilted substrate surfaces. Such nano-dimensional etching patterns have been observed for the wet chemical etching of sputtered AZO films when HF is also used as an etchant along with HCl [17]. The rms roughness values were estimated from AFM images and it was found that the σ_{rms} of texture E (~56 nm) increased to ~66 nm with the addition of 500 nm AZO. The rms roughness further decreased to ~58 nm with 700 nm of AZO and then slightly increased to ~67 nm when the AZO thickness was 1000 nm. This kind of textures could be suitable for the growth of μc-Si and a-Si as it does not exhibit peaks or deep valleys that can create cracks in the microcrystalline silicon films. Moreover the crater diameter lies between 500 nm to 1 μm (Figure 4) and has large opening angles, which is reported to be adequate for thin film silicon solar cells [18, 19].

Texture S, with a high substrate roughness of σ_{rms} = 145 nm, was found to be porous and randomly etched (Figure 5(a)). The differences between textures E and S arise from the different metal deposition method as described in the AIT process section. The deposition of AZO over texture S resulted in a cauliflower-like morphology with smooth valleys and free from sharp peaks or edges. The high surface porosity of texture S should have significantly controlled the initial phase of the AZO growth over this texture. The nucleation of the AZO films might have started by filling the highly porous surface and then continued to grow into the bulk columnar phase. This might be the reason for the smooth and continuous transition of texture S/AZO interface as shown in the cross-sectional SEM images of Figure 6. This also explains the decrease in surface roughness from 145 nm for texture S to 80 nm for texture S with 700 nm of AZO. When the thickness of AZO was further increased to 1000 nm, the σ_{rms} was found to increase up to 92 nm. This increase in surface roughness may be due to the contribution of different crystal orientations as shown in Figure 7 for this sample (S+AZO3). The sample with 700 nm of AZO was showing lower σ_{rms} values than the 500 nm and 1000 nm samples for both textures and the reason for this behaviour is not yet clear.

The structure of the AZO samples was analysed by means of XRD measurements. Figure 7 shows the XRD patterns in logarithmic scale to emphasize the low intensity features of the different AZO layers deposited on smooth substrates and on both textures E and S. All samples were found to be polycrystalline and presented the most intense diffraction peak at around $2\theta = 34.4^{\circ}$, indicating a hexagonal wurtzite structure of ZnO with the c-axis perpendicular to the substrate and oriented preferentially along the [001] direction. By comparing the XRD pattern of three different thicknesses of AZO grown on smooth surfaces, only (002) and its second-order reflection (004) were observed. In the case of AZO films over textured substrates, a decrease in the intensity of (002) peak was observed with increase in roughness along with the appearance of other crystallographic peaks corresponding to (100), (102), and (101), probably due to the fact that the grains are turned as the substrate is not smooth, revealing other ZnO wurtzite orientations.

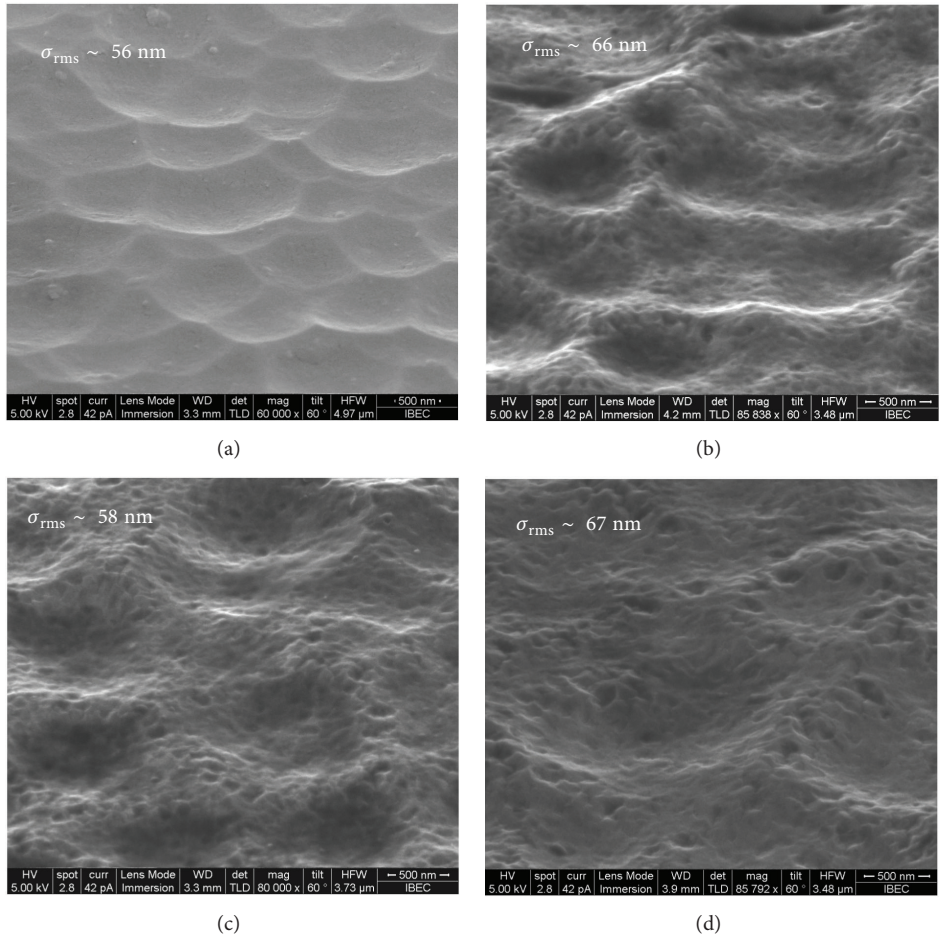

Figure 4: HRSEM (tilted at 60°) micrographs of (a) texture E, (b) E + AZO1 (500 nm), (c) E + AZO2 (700 nm), and (d) E + AZO3 (1000 nm). The σ_{rms} values were obtained from AFM.

The lattice parameter c was estimated from the position of the (002) peak, and all the films showed c parameter values very similar to that of undoped ZnO (c = 0.521 nm) [20]. The average crystallite sizes in the direction normal to the reflecting planes of AZO films over the smooth substrates showed values ~60 nm, and this is because these films were deposited under identical conditions which differ only in thickness. The average crystallite size of the films deposited on textured substrates was 38 ± 5 nm. This difference in the crystallite size and the appearance of the additional crystallographic peaks for the textured substrates indicate that the growth of AZO over randomly nanotextured substrates is quite different than on the smooth substrates. The films over the smooth substrates are highly preferentially oriented along the (002) direction; whereas when AZO films are deposited over the textured substrates, the initial nucleation of the films occurs at the tittered and porous surfaces and this might have led to a strained columnar growth. This is more predominant in the case of texture S with high surface roughness and resulted in showing different crystallographic growth orientations.

The surface roughness values and electrical and optical properties of the AZO deposited samples are summarised in Table 1. The resistivity of the AZO samples (average $\rho \sim 5.6 \times 10^{-4}$ Ω·cm) over smooth substrate did not show any significant difference since they were deposited under the same conditions; moreover, the average crystallite size values were also the same (~60 nm). AZO deposited over texture E showed resistivity values (~7×10^{-4} Ω·cm) slightly higher than those on smooth samples. Texture E presented very smooth craters and its texture might not have critically influenced the AZO growth. The resistivity of the AZO films on texture S showed higher values of ~10^{-3} Ω·cm. One of the electrical limiting transport mechanisms is the grain boundary potential barrier, and less grain boundaries means better conductivity. The presence of different crystal planes in the AZO films over texture S compared to the other samples suggests the existence of larger number of grain boundaries, and this might have resulted in the high resistivity of these samples.

The haze ratios of the AZO coated substrates are plotted in Figures 8(a) and 8(b) for texture E and texture S, respectively, along with those of the commercially available Asahi-U TCO. The integrated transmittance in the wavelength 400 to 800 nm and the calculated haze values at 600 nm of the

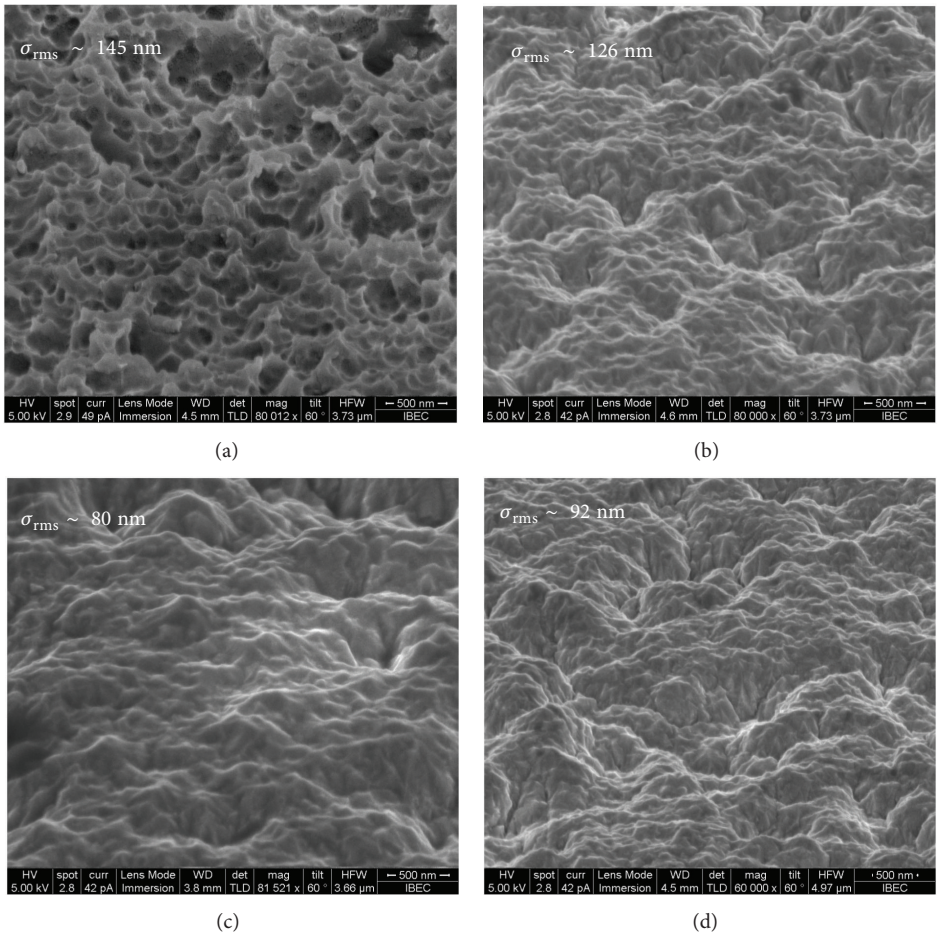

(a) (b) (c) (d)

Figure 5: HRSEM (tilted at 60°) micrographs of (a) texture S, (b) S + AZO1 (500 nm), (c) S + AZO2 (700 nm), and (d) S + AZO3 (1000 nm). The σ_{rms} values were obtained from AFM.

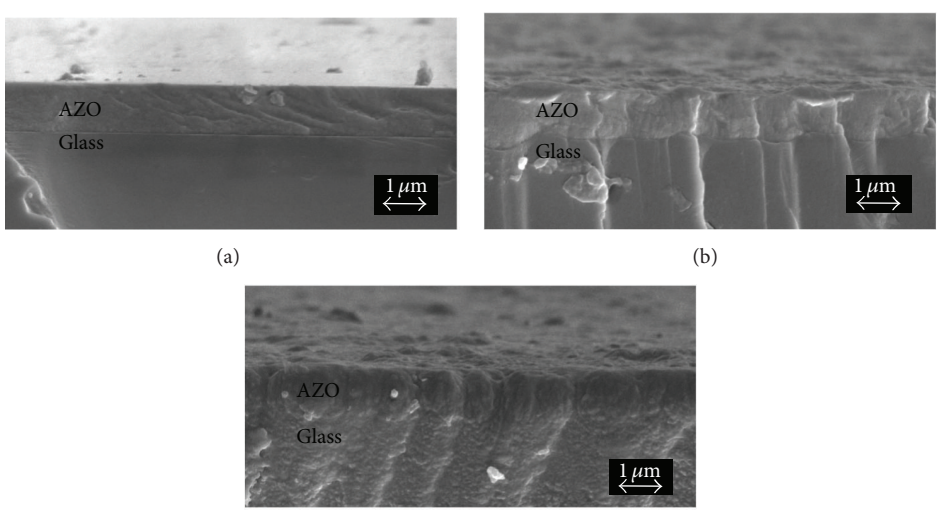

(a) (b) (c)

Figure 6: Cross-sectional SEM micrographs of AZO3 deposited on (a) smooth glass, (b) texture E, and (c) texture S.

Table 1: Surface roughness (σ_{rms}), resistivity (ρ), sheet resistance (R_s), integrated transmittance T (400–800 nm), haze at 600 nm, and figure of merit values (Φ) of the AZO layers deposited on smooth and textured glass along with that of Asahi-U substrate.

Sample	σ_{rms} (nm)	ρ (Ω·cm)	R_s($\Omega/\square$)	Integrated $T_{(400-800\,nm)}$ (%)	Haze at 600 nm (%)	$\Phi_{(400-800\,nm)}$ ($10^{-3}\ \Omega^{-1}$)
AZO1 (500 nm)	5	5.6×10^{-4}	11.2	84.5	—	16.5
AZO2 (700 nm)	7	5.9×10^{-4}	8.4	84.5	—	22.1
AZO3 (1000 nm)	9	5.3×10^{-4}	5.3	81.8	—	25.4
E + AZO1	66	7.1×10^{-4}	14.2	84.5	13.7	13
E + AZO2	58	6.9×10^{-4}	9.8	84.5	10.7	19
E + AZO3	67	7.0×10^{-4}	7	81.6	14.1	18.8
S + AZO1	126	1.2×10^{-3}	23	75.5	43.7	2.6
S + AZO2	80	1.2×10^{-3}	16.5	75.9	32.5	3.8
S + AZO3	92	9.5×10^{-4}	9.5	73.5	33.1	4.9
Asahi-U	25	—	9.3	78.3	10.1	9.4

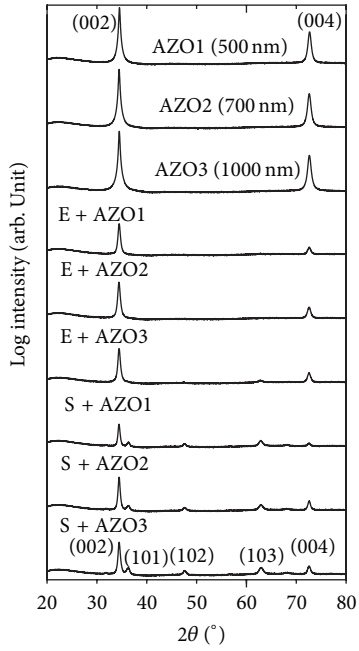

Figure 7: XRD patterns of the AZO films deposited over smooth and textured glasses.

AZO coated samples are given in Table 1. The haze at 600 nm wavelength showed a similar trend as that of roughness values, where the samples with 700 nm AZO showing the lower values for both textures E and S. A very high haze of ~33% at 600 nm was achieved for the texture S samples. The high haze in the wavelength range 600 to 1200 nm is highly beneficial for the light trapping in a-Si/μ-cSi solar cells.

More detailed understanding of the surface roughness can be extracted using the frequency distribution analysis of the roughness obtained by the Fourier transform of the AFM images. The power spectral density (PSD) function is the frequency spectrum of the surface roughness measured in inverse length and gives information about the periodicity and amplitude of the roughness. By using AFM images of $15 \times 15\,\mu m^2$, the PSD functions have been extracted from the AFM software and are plotted in Figure 9 for texture E and S along with that of Asahi-U as the reference (orange-squared symbols). The PSD at low spatial frequencies reflects the large lateral feature sizes that will contribute to lower-angle scattering and the PSD at high spatial frequencies is the result of a surface with small feature sizes which gives the large-angle light scattering [21]. Samples on texture E and S exhibit higher PSD values than Asahi-U, especially in the low spatial frequency range and this indicates their superior light scattering capability. This also means that these textures possess both small and larger feature sizes which can be confirmed by looking at the HRSEM images (Figures 4 and 5), where in all cases a superposition of a microtexture and a nanotexture can be observed.

The desired sheet resistance value of the TCO for the application as front contact in thin film silicon solar cells is ~ 10 $\Omega/\square$. Among the different samples reported here, the sheet resistance showed a tendency to increase with the surface roughness of glass. By considering the samples coated with same thickness of AZO, texture S showed sheet resistance values almost twice the corresponding one on smooth substrate. This high value of sheet resistance is a direct consequence of the increase in resistivity of these samples as mentioned earlier. An AZO thickness of nearly 1000 nm was necessary to get a sheet resistance lower than 10 $\Omega/\square$ for texture S and they showed a remarkable high haze value ~33% at 600 nm, but the transparency dropped to 73.5%. The low transmittance values of these samples compared to the AZO on smooth or texture E samples can be accounted for the very porous nature of texture S which could have formed void regions of low refractive index resulting in the reflection losses. Commercially available Asahi-U substrate shows a sheet resistance of 9.3 $\Omega/\square$, transmittance of 78.3%, and a haze value of 10% at 600 nm. Though texture S with 1000 nm AZO shows very high haze and good sheet resistance compared to Asahi-U, their transmittance is nearly 5% lower. Texture E sample with 700 nm AZO showed high transmittance of 84.5%, haze value of 10.7%, and a low sheet resistance of 9.8 $\Omega/\square$, which are comparable to those of Asahi-U. Texture E with 1000 nm AZO showed 81.5% transmittance with a high haze ~14% and a very low sheet resistance of 7 $\Omega/\square$.

In order to probe the effectiveness of the glass texture on the optical absorption in an a-Si solar cell, 200 nm of

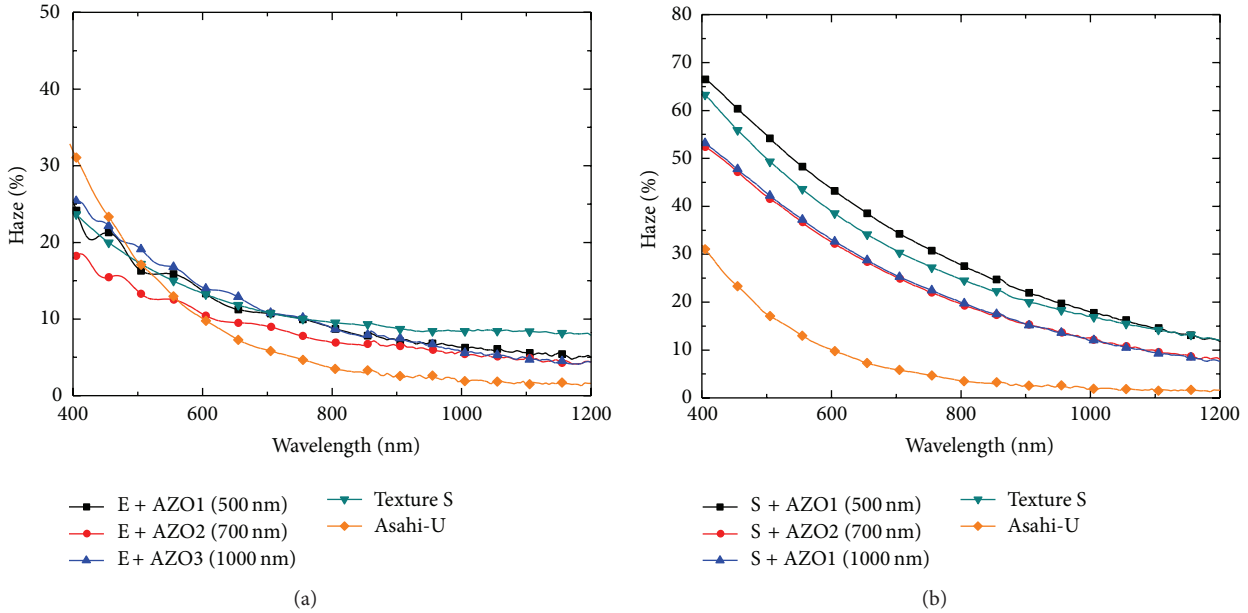

FIGURE 8: Haze values of the samples (a) texture E, texture E + three different AZO thicknesses, and Asahi-U substrate and (b) texture S + three different AZO thicknesses and Asahi-U substrate.

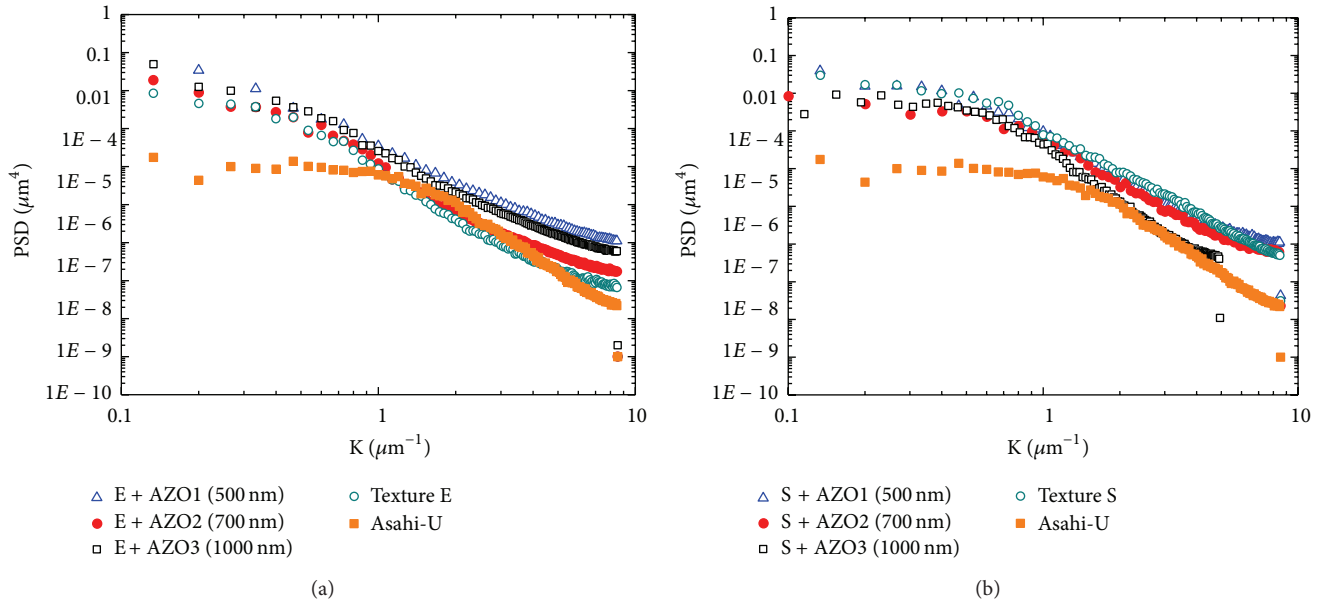

FIGURE 9: PSD plots for (a) texture E, E + AZO1, E + AZO2, E + AZO3, and Asahi-U and (b) texture S, S + AZO1, S + AZO2, S + AZO3, and Asahi-U.

a-Si:H were deposited over AZO3 coated texture E, texture S, and on smooth glass, followed by a 300 nm of Ag layer. The absorption spectra $(1 - R)$ of these samples (textured glass/AZO/a-Si:H/Ag) in the wavelength range 350 to 800 nm are compared in Figure 10. The high absorption region below 800 nm is due to the optical band gap absorption of a-Si which has band gap energy of ~1.74 eV. It can be noticed that the oscillations due to thin film interferences disappear for the textured surfaces and the absorbance in this range (350–800 nm) is highly improved in comparison to the smooth glass. The calculated figure of merit (FOM) values for TCOs on the smooth and textured glass are also given in Table 1. FOM is an estimation of the quality of the TCO based on the transmittance and electrical properties, and the higher the FOM is, the better is the TCO. AZO deposited on smooth glass substrates showed the high FOM values, whereas AZO on texture S showed the lowest values. But when the absorption ratio of the increase in the device is considered as shown in Figure 10, the texture S showed the highest absorption. Hence, it can be concluded that FOM

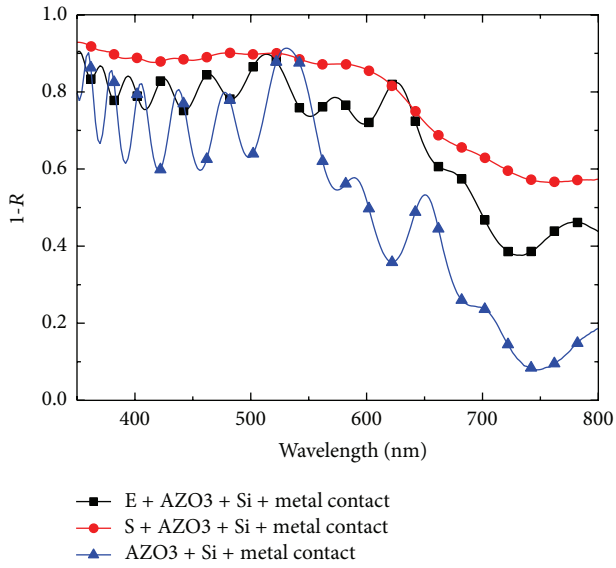

FIGURE 10: $(1 - R)$ spectra for smooth glass, texture E, and texture S with AZO3/a-Si:H (200 nm)/Ag.

is not a qualifying property to be addressed for the light scattering efficiency of a TCO in a solar cell, whereas the haze value plays the decisive role. The samples on texture E and texture S showed an increase in absorption (increase in absorption for textured device to the absorption for smooth one) of 35% and 53%, respectively, compared to those on the smooth glass. The texturing at the glass/TCO in combination with the modulated texture at AZO/a-Si interfaces results in an improved optical scattering yielding a higher absorption.

4. Conclusion

In this work, two different types of glass textures have been achieved depending on the Al deposition method and it has been demonstrated that one of the decisive factors to tune the texture roughness in AIT process is the method of deposition of the Al over the glass. The higher energy with which the adatoms reach the substrate surface during the sputtering deposition process gives better adhesion and compactness to the sputtered Al film and produced rougher textures during AIT process in comparison to the thermally evaporated films. The softer texture E ($\sigma_{rms} \sim 56$ nm) obtained from the evaporated Al showed smooth U-shaped craters (0.5 to 1 μm), whereas the sputtered films resulted in very rough and porous texture S ($\sigma_{rms} \sim 145$ nm). AZO over texture E showed U-shape craters with excellent electrical properties ($\rho \sim 7 \times 10^{-4}$ Ω·cm), haze values above 10% at 600 nm, and high transparency ($T_{(400-800\,nm)} > 81\%$), whereas AZO on texture S showed cauliflower-like surface. Though they showed high haze values (>30% at 600 nm) and transmittance values above 73%, an AZO thickness of 1000 nm was necessary to obtain a sheet resistance value below 10 Ω/□. The efficiency of these textures in light trapping was evaluated by fabricating the device structure, *textured glass/AZO/a-Si:H/Ag*, using textures E, S, and smooth glass. Absorption enhancements of 33% and 55% were obtained for textures E and S compared to those on the smooth glass, confirming their ability to enhance the light absorption in silicon thin film solar cells to gain higher short circuit current.

Conflict of Interests

The authors declare that there is no conflict of interests regarding the publication of this article.

Acknowledgments

This work has been supported by the Ministerio de Economía y Competitividad and the European Regional Development Fund through the projects AMIC (ENE2010-21384-C04-03) and INNDISOL (IPT-420000-2010-6).

References

[1] J. Müller, B. Rech, J. Springer, and M. Vanecek, "TCO and light trapping in silicon thin film solar cells," *Solar Energy*, vol. 77, no. 6, pp. 917–930, 2004.

[2] S. Faÿ, J. Steinhauser, S. Nicolay, and C. Ballif, "Polycrystalline ZnO: B grown by LPCVD as TCO for thin film silicon solar cells," *Thin Solid Films*, vol. 518, no. 11, pp. 2961–2966, 2010.

[3] Z. Remes, M. Vanecek, H. M. Yates, P. Evans, and D. W. Sheel, "Optical properties of SnO_2:F films deposited by atmospheric pressure CVD," *Thin Solid Films*, vol. 517, no. 23, pp. 6287–6289, 2009.

[4] O. Kluth, B. Rech, L. Houben et al., "Texture etched ZnO:Al coated glass substrates for silicon based thin film solar cells," *Thin Solid Films*, vol. 351, no. 1-2, pp. 247–253, 1999.

[5] N. Chuangsuwanich, P. Campbell, P. I. Widenborg, A. Straub, and A. G. Aberle, "Light trapping properties of evaporated poly-silicon films on ait-textured glass substrates," in *Proceedings of the 31st IEEE Photovoltaic Specialists Conference*, pp. 1161–1164, January 2005.

[6] G. Jin, P. I. Widenborg, P. Campbell, and S. Varlamov, "Lambertian matched absorption enhancement in PECVD poly-Si thin film on aluminum induced textured glass superstrates for solar cell applications," *Progress in Photovoltaics: Research and Applications*, vol. 18, no. 8, pp. 582–589, 2010.

[7] J. Wang, S. Venkataraj, C. Battaglia, P. Vayalakkara, and A. G. Aberle, "Analysis of optical and morphological properties of aluminium induced texture glass superstrates," *Japanese Journal of Applied Physics*, vol. 51, no. 10, Article ID 10NB08, 2012.

[8] P. I. Widenborg and A. G. Aberle, "Polycrystalline silicon thin-film solar cells on AIT-textured glass superstrates," *Advances in OptoElectronics*, vol. 2007, Article ID 24584, 7 pages, 2007.

[9] H. Cui, M. A. Green, P. R. Campbell, M. J. Wolff, and G. Jin, "Enhanced absorption of SPC poly-si thin films on aluminium induced textured (AIT) glass with submicron texture feature size," in *Proceedings of the 25th EU PVSEC/5th World Conference on Photovoltaic Energy Conversion (WCPEC '10)*, pp. 3691–3694, Valencia, Spain, September 2010.

[10] G. Haacke, "New figure of merit for transparent conductors," *Journal of Applied Physics*, vol. 47, no. 9, pp. 4086–4089, 1976.

[11] W. van Gelder and V. E. Hauser, "The etching of silicon nitride in phosphoric acid with silicon dioxide as a mask," *Journal of the Electrochemical Society*, vol. 114, no. 8, pp. 869–872, 1967.

[12] N. H. Ray, "The action of phosphoric acid on glass," *Journal of Non-Crystalline Solids*, vol. 5, no. 2, pp. 71–77, 1970.

[13] B. N. Chapman, "Thin-film adhesion," *Journal of Vacuum Science and Technology*, vol. 11, no. 1, pp. 106–113, 1974.

[14] M. Ohring, *The Materials Science of Thin Films*, Academic Press, Boston, Mass, USA, 1991.

[15] O. Kluth, G. Schöpe, J. Hüpkes, C. Agashe, J. Müller, and B. Rech, "Modified Thornton model for magnetron sputtered zinc oxide: film structure and etching behaviour," *Thin Solid Films*, vol. 442, no. 1-2, pp. 80–85, 2003.

[16] A. M. Rosa, E. P. da Silva, E. Amorim et al., "Growth evolution of ZnO thin films deposited by RF magnetron sputtering," *Journal of Physics: Conference Series*, vol. 370, no. 1, Article ID 012020, 2012.

[17] J. I. Owen, J. Hüpkes, H. Zhu, E. Bunte, and S. E. Pust, "Novel etch process to tune crater size on magnetron sputtered ZnO: Al," *Physica Status Solidi A*, vol. 208, no. 1, pp. 109–113, 2011.

[18] M. Python, O. Madani, D. Dominé, F. Meillaud, E. Vallat-Sauvain, and C. Ballif, "Influence of the substrate geometrical parameters on microcrystalline silicon growth for thin-film solar cells," *Solar Energy Materials and Solar Cells*, vol. 93, no. 10, pp. 1714–1720, 2009.

[19] M. Berginski, J. Hüpkes, M. Schulte et al., "The effect of front ZnO:Al surface texture and optical transparency on efficient light trapping in silicon thin-film solar cells," *Journal of Applied Physics*, vol. 101, no. 7, Article ID 074903, 2007.

[20] JCPDS card No 36-1451.

[21] N. Sahraei, K. Forberich, S. Venkataraj, A. G. Aberle, and M. Peters, "Analytical solution for haze values of aluminium-induced texture (AIT) glass superstrates for a-Si:H solar cells," *Optics Express*, vol. 22, no. 1, pp. A53–A67, 2014.